

ELECTROCHEMICAL EVALUATION OF THE RELATIONSHIP BETWEEN THE THERMAL TREATMENT AND THE PROTECTIVE PROPERTIES OF THIN SILICA COATINGS ON ZINC SUBSTRATES

TAMARA-RITA OVÁRI^a, GABRIEL KATONA^b, GABRIELLA SZABÓ^{b,*},
LIANA MARIA MURESAN^a

ABSTRACT. One of the challenges of smart and thin silica layers preparation on metallic substrates consists in the simultaneous network formation and introduction of corrosion inhibitors in it. Taking into account that both steps are affected by the temperature, it is really important to evaluate first its effect on the silica network formation. In this context, this paper aims the presentation of findings regarding the optimal heat treatment parameters in the preparation of thin silica (SiO_2) coatings on zinc. These silica layers were prepared by sol-gel method (dip-coating technique) and were tested as protective films against zinc (Zn) corrosion. After optimization of several parameters such as the drying temperature, drying duration, the corrosion resistance of the coatings was evaluated mainly by means of electrochemical methods (electrochemical impedance spectroscopy and potentiodynamic polarization). The electrochemical evaluation corroborated with morpho-structural characterization led to the conclusion that the SiO_2 coatings have better protection properties when dried at 150°C for 1h.

Keywords: zinc; sol-gel; silica coating; electrochemical impedance spectroscopy; potentiodynamic polarization curves

INTRODUCTION

Materials-oriented scientists manifest great interest in the last decades towards sol-gel techniques and coatings preparation on different substrates.

^a Department of Chemical Engineering, Babes-Bolyai University, Faculty of Chemistry and Chemical Engineering, 11, Arany J. St, 400028 Cluj-Napoca, Romania

^b Department of Chemistry and Chemical Engineering of Hungarian Line, Babes-Bolyai University, Faculty of Chemistry and Chemical Engineering, 11, Arany J. St, 400028 Cluj-Napoca, Romania

* Corresponding author: gabriella.szabo@ubbcluj.ro

The sol-gel route is based on the evolution of a colloidal system through the formation of an inorganic or hybrid sol followed by its gelation to form a continuous polymer network (gel) [1]. Among these, due to their versatile applications, silica thin films have a great importance. Some of them aim to obtain superhydrophobic, anti-fogging [2], antireflective and increased light transmitting [3, 4] surfaces applicable on solar cells, eyeglasses, windshields and other optical areas. The deposition of silica coatings on coked alumina refractories, units of the petrochemical industry, can modify their surface and enhance their mechanical properties [5]. Last but not least, an important application of silica layers is due to their anticorrosion protective properties.

The coatings prepared by sol-gel method showed great potential for the replacement of toxic pre-treatments and layers, like chromate conversion coatings, which have traditionally been used [6], but due to highly toxic hexavalent chromium salts, which cause DNA damage and cancer [1], they were banned [7, 8]. This method is an eco-friendly technique of metal surface protection against corrosion and offers many advantages, a few of them being the low processing temperature and the “green” coating technology, which means that the method is waste-free and excludes the stage of washing [6]. Sol-gel coatings act as barriers on the surface of the metal, blocking the access of corrosive media and enhancing the corrosion protection [9, 10]. Despite the fact that wide-ranging studies were made in the past decades, the relationship between the sol formation, gelation process parameters and the interface properties of these coatings are not very well known yet. To control and design the properties of these coatings, further studies are necessary [6]. The sol composition (molar ratio of components), the used solvent and catalyst (acid or base), the ageing and annealing temperature, and the thermal treatment duration are factors that determine the structure and subsequently the mechanical and optical properties, as well as the electrochemical resistance [2-5, 11] of the coatings.

In previous works, we reported the preparation of mesoporous silica coatings by sol-gel method and the impregnation of their pore system with corrosion inhibitors [12, 13]. In other cases, they were doped with encapsulated corrosion inhibitors and polymerizable agents and consequently they exhibited self-healing properties [14-18].

In the cases of mesoporous coatings, surfactants were added to the precursor sols in higher concentration than the critical micellar concentration. By the heat treatment, the as formed micelles were transformed into pores that could host corrosion inhibitors. However, there are several nanoparticles (e.g., graphene oxide GO) that cannot be introduced in the mesopores formed in the abovementioned way, so in those cases this procedure is useless. From this perspective there is no need for the heat treatment at 410 °C mentioned in our

previous reports which was necessary only for the combustion of the micelles. In case of Zn, a supplementary complication occurs due to its behavior at elevated temperatures, more specifically exceeding 200 °C, when horizontal and vertical cracks could appear on the metal surface [19]. It also has a melting point of 419.5 °C. This is why a reconsideration of the thermal treatment of the silica coatings is necessary.

Although it has a broad implementation, the heat treatment of silica coatings differs from one study to another [7, 9, 10] and from one metal to another. As it is of great importance to generate excellent adhesion between the Zn surface and silica coating, the influence of the temperature and its effects on the silica layers deposited on Zn needs to be further discussed. Moreover, in our previous work, aiming to develop a coating with both barrier and inhibitor carrier properties, it was reported that compact silica layers on Zn presented approximately the same anti-corrosive protection like the porous ones, which were obtained at higher temperatures [12]. This interesting and unexpected finding motivated the further investigation on how the thermal treatment affects the silica coatings properties

In this work, a detailed investigation regarding the curing process of the silica coating was made to determine the optimal conditions (drying temperature and duration) for the preparation of silica coatings on zinc substrates by sol-gel method. To the best of our knowledge, a deep electrochemical investigation able to correlate the anti-corrosion properties of the coatings with the thermal treatment parameters of silica deposits on zinc was not yet reported. For this purpose, electrochemical impedance spectroscopy (EIS) and potentiodynamic polarization measurements were used. The morphology and structure of the silica were determined by SEM, and the thickness of the layer by AFM measurements.

RESULTS AND DISCUSSION

The corrosion protective properties of silica-coated zinc samples prepared in different experimental conditions (various drying temperatures and drying times) were tested in an aqueous solution of 0.2 g/l Na₂SO₄ (pH 5) by using electrochemical investigation methods.

Influence of drying temperature

In order to choose properly the drying temperature of the silica coatings, firstly, thermogravimetric analysis was performed. During the probe heating, it was noticed a total loss of 86,6% in a single step. (TG). This was attributed

to the evaporation of the ethylic alcohol at 59°C (DTG supplementary data are available upon request from the authors). Therefore, the first annealing temperature (a little bit higher than the solvent evaporation) was chosen to be 80°C. On the other hand, in order to avoid the coating deterioration, the highest drying temperature was limited to 350°C. Next, several experiments were carried out in the interval between 80°C and 350°C in order to determine the optimal drying temperature of the silica protective coatings. All the coatings described in this study showed a glassy and transparent visual aspect.

Figure 1 presents the Nyquist diagrams obtained for the samples dried at ambient temperature, 80°C, 150°C, 200°C and 350°C for 0.5h, respectively, recorded at OCP. At first sight, the largest diameter of the capacitive loop, which can be assigned to the polarization resistance (R_p), was noticed in the case when the protective layer was dried at 150°C. An inductive loop was observed at 350°C suggesting a change of the protection mechanism offered by the coating.

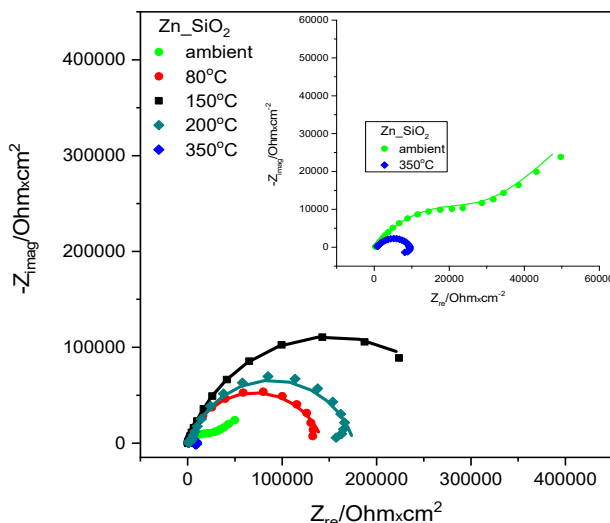


Figure 1. Nyquist impedance spectra of compact SiO_2 layers on zinc substrate dried at different temperatures for 0.5 hours. Samples were immersed in Na_2SO_4 electrolyte pH =5; spectra were recorded in 10 mHz –100 kHz frequency range.

Insets: spectra of coated Zn dried at ambient temperature and 350 °C

Impedance data were modelled using three different electrical circuits presented in **Figure 2**. The corresponding parameters obtained after fitting the experimental diagrams to an equivalent electrical circuit model are listed in **Table 1**. In all the cases, the accuracy of the fitting was estimated with the

relative standard error percent for the equivalent circuit parameters (mostly below 10%) and the chi-squared χ^2 value (around 10^{-3} or less). In **Figure 2**, R_s is the solution resistance, R_{ct} and Q_{dl} represent the charge transfer resistance and the constant phase element corresponding to the electrical double layer capacitance at the metal/solution interface, R_{coat} and C_{coat} are the coating resistance and capacitance, respectively, and L and R (**Figure 2C**) are the inductance and the resistance occurring when the coating was heated at high temperatures during drying, suggesting a structural change of the coating.

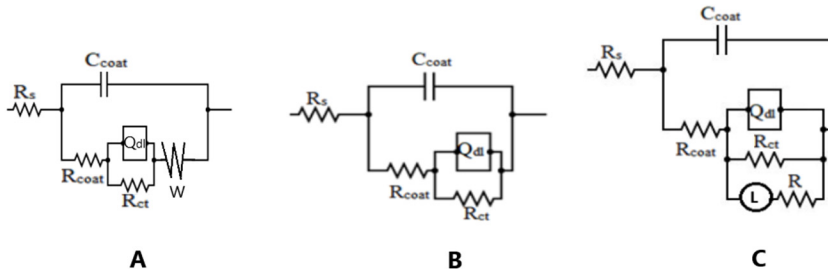


Figure 2. Equivalent electrical circuits used to model the metal/electrolyte interface when the silica coating was dried at temperatures: ambient (A), 80 °C – 200 °C (B) and at 350 °C (C)

In the case of drying at ambient temperature, the Warburg impedance in **Figure 2A** could be attributed to the diffusion of ions through the incompletely formed silica layer on zinc surface in which the polycondensation process continues taking place, as it is not finished at the moment of metal extraction from the gel and after drying it at low temperature.

Table 1. Electrochemical parameter values for Zn/SiO₂ coated samples calculated by non-linear regression of the impedance data using the equivalent electrical circuits from **Figure 2**. (n~0.79)

Temp. °C	R_s (kΩ·cm ²)	C_{coat} (μF/cm ²)	R_{coat} (kΩ·cm ²)	Q_{dl} (μSs ⁿ /cm ²)	R_{ct} (kΩ·cm ²)	$10^4 \cdot W$ (Ss ⁵ /cm ²)	$10^{-5} L$ (H·cm ²)	R (kΩ·cm ²)	R_p (kΩ·cm ²)
ambient	0.35	0.154	0.25	1.67	24.61	1.213	-	-	-
80	0.14	0.328	0.16	5.55	143.10	-	-	-	143.26
150	0.17	0.268	0.202	4.83	304.8	-	-	-	305.00
200	0.61	0.085	2.61	2.67	172.80	-	-	-	175.41
350	0.69	0.036	0.24	6.66	8.80	-	4.033	17.9	9.04

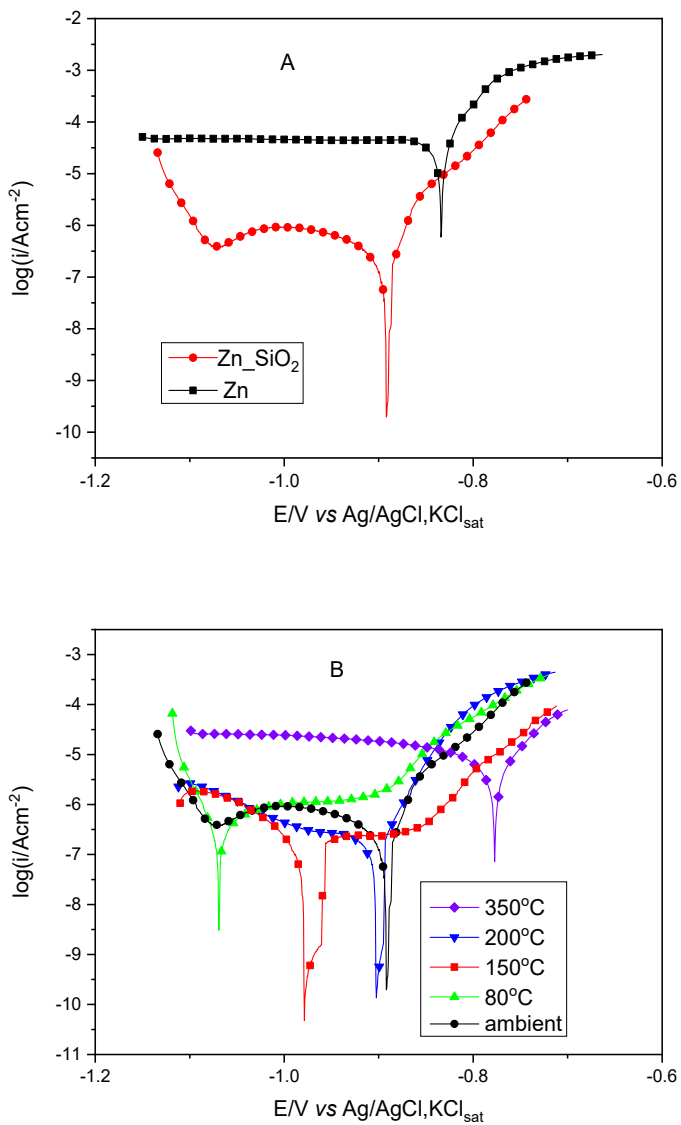


Figure 3. Potentiodynamic polarization curves recorded for bare Zn and Zn/SiO₂ samples at ambient temperature (A) and Zn/SiO₂ samples thermally treated at different temperatures (ambient, 80 °C, 150 °C, 200 °C and 350 °C) for 0.5 h (B)

The appearance of an inductive loop at high temperatures could be associated with the variation of the active surface area of the electrode and can be ascribed to an adsorbed intermediate relaxation. This type of behaviour was observed in other corroding systems too [22]. At these temperatures, also possible cracks may appear which explain the lower corrosion resistance of the coating (see also **Figure 8**). The results are similar with those reported previously in literature [1].

Further investigations were conducted by recording the potentiodynamic polarization curves of the various coated Zn samples heated at different temperatures (**Figure 3**). Bare Zn samples were used for comparison.

Some kinetic parameters like corrosion potential (E_{corr}), anodic (β_a) and cathodic (β_c) coefficients (representing the slopes of the fitted plots) were obtained by the Tafel interpretation of the polarization curves. The Tafel plots should be considered only an approximate evaluation method for the corrosion of coated metals, because the coatings themselves should be protective and are supposed to corrode only at pores. Nevertheless, the information extracted from the curves can give useful preliminary information about the corrosion resistance of the coatings [23].

$$i_{corr} = \frac{\beta_a \cdot \beta_b}{2.303 \cdot R_p \cdot (\beta_a + \beta_b)} \quad (1)$$

where β_a and β_c are the Tafel slopes determined from the polarization curves and R_p is the polarization resistance obtained from the impedance spectra.

For all samples, the kinetic parameters obtained by Tafel interpretation (the corrosion potential E_{corr} , cathodic and anodic Tafel coefficients β_c and β_a) are listed in **Table 2**. The corrosion current densities i_{corr} were calculated by Stern-Geary equation, the polarization resistance values (R_p) were determined from impedance spectra. PE represents protective efficiency.

Table 2. Corrosion parameters for coated zinc samples determined from Tafel interpretation of the polarization curves from **Figure 3**.

Sample	T °C	E_{corr} (vs. Ag/AgCl, KCl) (V)	i_{corr} ($\mu\text{A} / \text{cm}^2$)	β_c (V/dec)	β_a (V/dec)	R_p ($\text{k}\Omega \cdot \text{cm}^2$)	PE (%)
Bare Zn	ambient	-0.830	16.030	-	0.048	1.30	-
Zn/SiO ₂	ambient	-0.891	0.526	0.216	0.035	24.86	96.72
	80	-1.068	0.078	0.031	0.149	143.26	99.51
	150	-1.040	0.090	0.080	0.300	305.00	99.44
	200	-0.901	0.087	0.280	0.040	175.41	99.45
	350	-0.766	2.86	0.489	0.068	9.04	82.16

The protective efficiency of the coatings, PE, was calculated with the formula:

$$PE(\%) = 100 \cdot \frac{i_{corr}^0 - i_{corr}}{i_{corr}^0} \quad (2)$$

where i_{corr}^0 is the value of the corrosion current density for the uncoated Zn sample, while i_{corr} is the corrosion current density of the coated samples.

The random change in the Tafel constants indicates a mixed inhibition mechanism where rates of zinc dissolution (anodic process) and oxygen evolution (cathodic process) are retarded by the presence of sol-gel coatings [24].

Analyzing the polarization curves, it can be also seen that a decrease with three orders of magnitude of i_{corr} is noticed (in comparison with the bare Zn) in the case when the drying temperature was 150°C. In this case, the protection efficiency reached 99.64 % suggesting that the coating is continuous, without cracks and able to protect successfully the zinc substrate. Consequently, for further experiments, the optimal drying temperature was chosen 150°C.

Influence of heat treatment duration

After preparation, the coated samples were heated at the optimal drying temperature (150 °C) in a drying oven for 0.5 h, 1 h, 2 h and 4 h. The Nyquist impedance spectra from **Figure 4** show the largest diameter of the capacitive loop corresponding to the polarization resistance at the duration of 1h of the drying process. It is believed that at this time the silica's polycondensation is finished. After 4h, further heating of the coating could lead to structural changes that are not beneficial for the coating's resistance (cracks may appear).

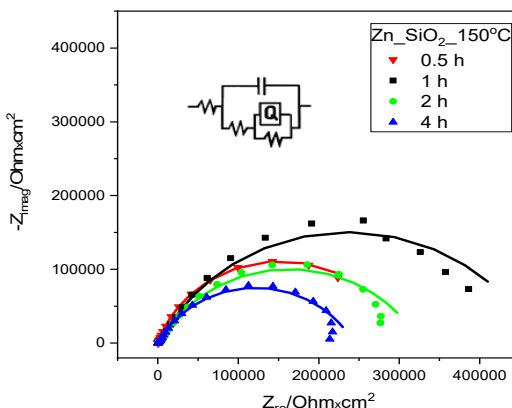


Figure 4. Nyquist impedance spectra of compact SiO₂ layers on zinc substrate prepared at 150°C with different duration of heat treatment. Samples were immersed in Na₂SO₄ electrolyte pH =5, spectra were recorded in 10 mHz –100 kHz frequency range.

The EIS spectra were fitted to the equivalent electrical circuit model from **Figure 2B** and the results are presented in **Table 3**.

Table 3. Electrochemical parameter values for Zn/SiO₂ coated samples dried at 150°C for different intervals of time calculated by non-linear regression of the impedance data. (n~0.79)

Heat treatment duration (h)	R _s (kΩ·cm ²)	C _{coat} (μF/cm ²)	R _{coat} (kΩ·cm ²)	Q _{dl} (μSs ⁿ /cm ²)	R _{ct} (kΩ·cm ²)	R _p = R _{coat} + R _{ct} (kΩ·cm ²)	X ²
0.5	0.17	0.268	0.20	4.83	304.80	305.00	1.74·10 ⁻³
1	0.58	0.084	2.37	3.89	468.20	470.57	7.12·10 ⁻³
2	0.73	0.085	1.66	3.57	323.60	325.26	5.35·10 ⁻³
4	0.21	0.107	0.78	3.12	242.80	243.58	3.52·10 ⁻³

It can be observed that the highest resistance of the coating was reached after 1h. In the same time, the charge transfer resistance R_{ct} reaches a maximum, suggesting a braking of the corrosion process as compared to the coatings heated at lower or higher temperatures. This is due to better protective properties of the silica coating.

The polarization curves corresponding to the corrosion behaviour of Zn/SiO₂ samples heated at 150 °C for different intervals of time are presented in **Figure 5**.

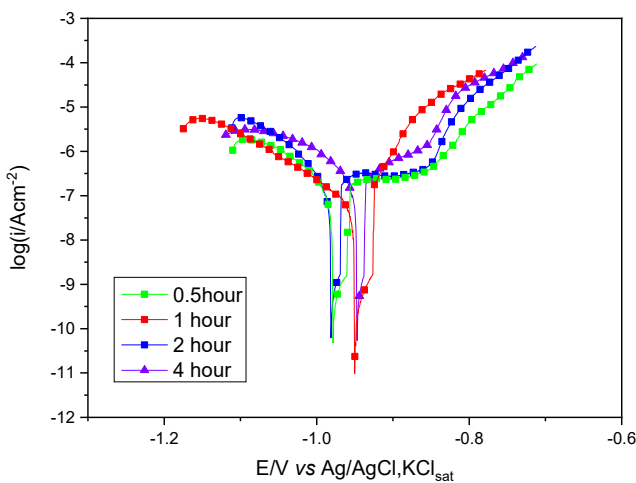


Figure 5. Potentiodynamic polarization curves recorded for zinc and Zn/SiO₂ samples heated at 150 °C for different intervals of time.

The kinetic parameters of the corrosion process obtained by the Tafel interpretation of the above-mentioned polarization curves are listed in **Table 4**. As before mentioned, E_{corr} is the corrosion potential, and β_c and β_a are the cathodic and anodic Tafel coefficients. The corrosion current densities i_{corr} were calculated by Stern-Geary equation, the polarization resistance values (R_p) were determined from impedance spectra. PE represents the protective efficiency.

Table 4. Corrosion parameters for coated zinc samples determined from Tafel interpretation of the polarization curves (**Figure 5**).

Heat treatment	Duration	E_{corr} (V vs. RE)	i_{corr} ($\mu\text{A} / \text{cm}^2$)	β_c (V/dec)	β_a (V/dec)	R_p ($\Omega \cdot \text{cm}^2$)	PE (%)
Bare Zn	-	-0.83	16.03	-	0.048	1.30	-
Zn/SiO ₂	0.5 h	-1.040	0.090	0.080	0.300	305.00	99.44
	1 h	-0.952	0.043	0.064	0.166	470.57	99.73
	2 h	-0.980	0.077	0.077	0.232	325.26	99.52
	4 h	-0.945	0.095	0.091	0.128	243.58	99.41

Analysing the parameters listed in **Table 4**, one can conclude that the best performance belongs to the coatings dried at 150 °C for 1h. This is in agreement with the results obtained with EIS method. The corrosion current densities reported in our previous works [9, 12] for compact silica coatings prepared at high temperature of 410 °C were μA order, similar to those obtained at 350 °C, but a significant current drop was achieved only by using a silylating agent. By using lower annealing temperatures, such as 150 °C it can be observed the decrease of i_{corr} with approximately two orders of magnitude without any further treatment.

Atomic force microscopy

In order to assess surface coverage and coating homogeneity, AFM analysis was conducted on Zn/SiO₂ samples. The atomic force microscopy images on the pre-treated bare zinc sample show a relatively uniform surface with only a few remaining scratches after the polishing procedure (**Figure 6 A and B**).

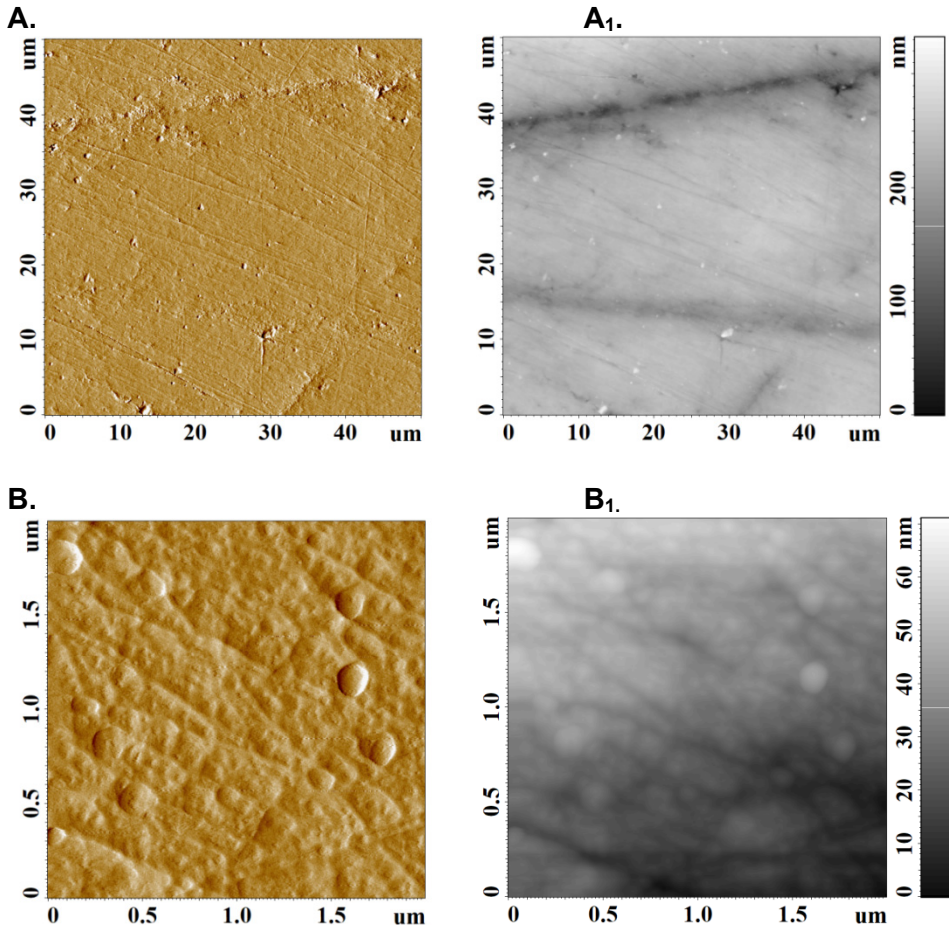


Figure 6. AFM images at two different magnifications (A, B) and high-resolution topographies (A1, B1) of Zn samples.

The high-resolution topographies prove that the depth of these surface deformities is generally below 60 nm, with only a few reaching 100 nm (**Figure 6 A1 and B1**). In the same time, from our previous studies regarding the coating thickness [9, 12] we learned that compact silica deposits are about 130 – 250 nm thin depending on the number of layers.

Similarly, AFM images of the coated surface point to a surface irregularity generally lower than 10 nm (**Figure 7 A1, B1**). Due to the effectiveness of the coating process, most surface deformities appear to be

covered by SiO_2 (**Figure 7A and B**), while only a few crevices with more significant depth remaining visible on the AFM images (**Figure 7 A**). Overall, microscopy studies point to a good coverage of the zinc surface.

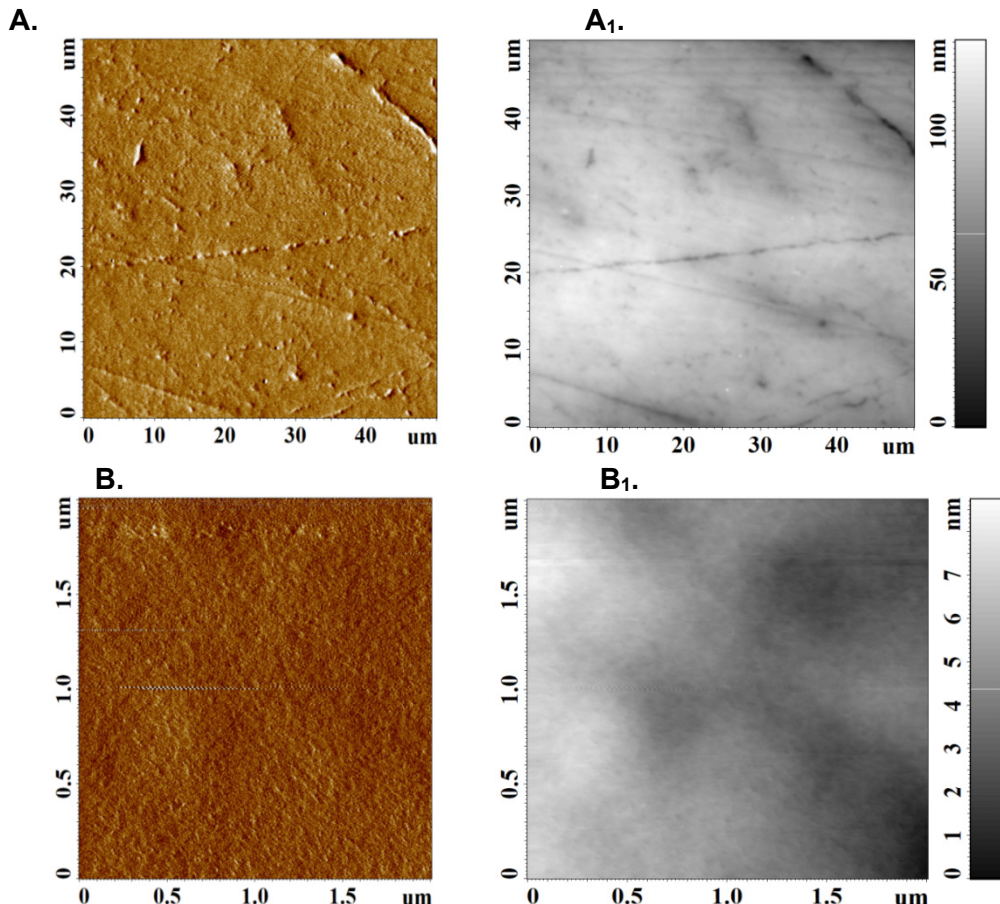


Figure 7. AFM images at two different magnifications (A, B) and high-resolution topographies (A1, B1) of Zn/SiO_2 samples dried at 150°C during 1h.

Scanning electron microscopy

SEM images taken immediately after the silica coating deposition on zinc and after 2 weeks held in a corrosive solution of Na_2SO_4 (pH 5) clearly showed that the heat treatment at 350°C causes the cracking of the silica coating from the beginning (**Figure 8 B and D**). These cracks explain the

lower corrosion protective efficiency of these layers (**Table 2**) [25]. On the contrary, the samples cured at 150 °C present a good coverage (**Figure 8 A**) and only few corrosion points even after 2 weeks of immersion in the corrosive medium (**Figure 8 C**).

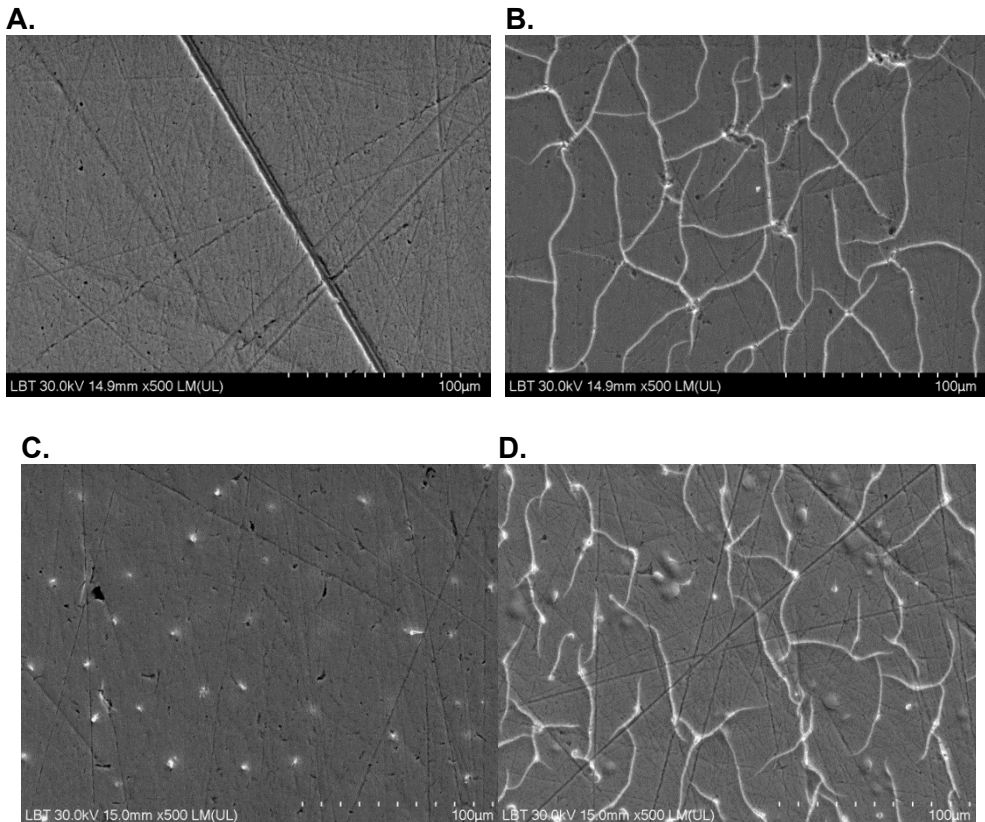


Figure 8. SEM images of silica coated Zn samples, thermal treated during 1 h after layer deposition at (A) 150 °C, and (B) 350 °C; after kept 2-weeks in 0.2 g/L Na₂SO₄ solution (pH 5) for sample treated at (C) 150 °C and (D) 350 °C.

CONCLUSIONS

The preparation of thin sol-gel silica coatings on zinc substrates was optimized in order to enhance their anti-corrosion properties. SiO₂ can improve the oxidation and acidic corrosion resistance of zinc due to its high heat and chemical resistance. After comparing the obtained results with that

of previous ones [12], one can conclude, that the heat treatment of the coatings between 80-200 °C caused an increasing anti-corrosion resistance, the corrosion current densities decreased approximately two orders of magnitude.

The duration of the heat treatment also influences the properties of layers, and it was shown that the optimal time interval is 1 hour. Results have shown to be very promising and led to the conclusion that the SiO₂ coatings have better protection properties when dried at 150°C for 1h. In these conditions can be obtained a quite compact, crack free and very good coverage of the Zn surface.

Nevertheless, the electrochemical measurements have shown that the investigated system, even when prepared in optimized conditions, exhibit only limited barrier properties and after a while the pitting corrosion appears. This drawback could be diminished by hydrophobization, multi-layer deposition and/or doping.

EXPERIMENTAL SECTION

Materials

Tetraethyl-orthosilicate (TEOS, for synthesis, >99%, Merck), hydrochloric acid (HCl, purum, 37%, Fluka), ethanol (EtOH, a.r., >99.7%, Reanal), and distilled water were used for preparing the precursor sol. The electrochemical measurements were done in aqueous solution of sodium sulfate (Na₂SO₄, 99%, Riedel-de Haen).

The Zn substrate (7x2cm) was polished emery paper (grade 1200, 2000, 3000), then ultrasonicated in 2-propanol (2-PrOH, a.r., > 99.7%, Reanal), cleaned with 0.1M aqueous HCl solution and with 2-propanol before layer deposition. The active surface of the sample in electrochemical measurements was limited to 2 cm².

Precursor sol synthesis

Silica precursor sols were prepared by acid catalysed, controlled hydrolysis of TEOS in ethanolic media. 0.1M aqueous HCl solution was used as a catalyst. The molar ratios for TEOS:EtOH:H₂O:HCl were 1:18.6:5.5:1 10⁻³ M. The solution was stirred for 60 min at ambient temperature. The precursor sols were stored at 25°C for 24 h prior to use [12].

Preparation of the coatings

Before layer deposition, in order to remove any scratches from the surface of the Zn substrate, it was polished with emery paper. In the subsequent step, the substrate was ultrasonicated in 2-propanol solution for

2 minutes, then treated with 0.1M aqueous HCl solution followed by 2-propanol solution and dried.

The sol-gel silica films on Zn were prepared from the above-mentioned precursor sol by dip-coating method (home-made dip-coater). The procedure consisted in the immersion of the cleaned and dried substrates in the precursor sol with a constant speed of withdrawal of 10 cm/min. The coated Zn was annealed at different temperatures (ambient temperature, 80°C, 150°C, 200°C, 350°C) for 0.5h or at 150°C at different drying durations (0.5h, 1h, 2h, 4h) with the aim of finding the optimal parameters to obtain favourable results consisting their anticorrosion properties.

Electrochemical characterization

The electrochemical measurements were carried out in a three-electrode cell containing a working electrode (the bare or coated Zn sample, S= 2 cm²), a counter electrode (platinum wire) and a reference electrode (Ag/AgCl/KCl_{sat}). All measurements were performed in 0.2 g/L Na₂SO₄ solution (pH = 5.0) with a computer-controlled potentiostat (PARSTAT 2737). First of all, the open circuit potentials (OCP) were recorded during 1 h and after that, electrochemical impedance spectroscopy (EIS) measurements were performed in the frequency range 10 mHz –100 kHz, with a sinusoidal current of 10 mV amplitude, at OCP. Further, the polarization curves (E = ± 200 mV vs. OCP) were recorded with a scan rate of 0.166 mV/s.

Atomic force microscopy analysis

The high-resolution topographies were recorded with an MFP-3D atomic force microscope (Asylum Research, Santa Barbara CA; driving software written in IgorPro 6.34A, Wavemetrics), using rectangular silicon cantilevers with a tetrahedral tip of a radius below 10 nm (AC240, Olympus, Optical Co. Ltd. Tokyo, Japan). The spring constant for each cantilever used was calibrated prior to measurements, according to standard built-in procedures [20, 21]. The images were recorded in a 50X50 μm and 2X2 μm surface area, respectively. All height images were first order flattened and plane-fitted in order to correct any sample tilt.

Scanning electron microscopy analysis

To study the morphological and structural properties of the coatings a Hitachi SU8230 ultra-high resolution scanning electron microscope was used. SEM measurements were conducted to investigate the surface morphology of the samples treated at high temperature such as 350 °C, compared with the samples cured on 150 °C for 1h.

Thermogravimetric investigation

In order to establish the right working temperature interval, thermogravimetric analysis of the silica gel was carried out on a TGA/SDTA 851e-METTLER, TOLEDO apparatus. The samples were placed in an Alumina 900 μ L sample holder. The measurements were carried out in a 60mL/min flow rate fed air atmosphere.

ACKNOWLEDGMENTS

The present work has received financial support through the project: Entrepreneurship for innovation through doctoral and postdoctoral research, POCU/380/6/13/123886 co-financed by the European Social Fund, through the Operational Program for Human Capital 2014- 2020. The authors thank Dr. Ioana Perhaiță for the thermogravimetric analysis.

REFERENCES

1. M. Zheludkevich; I.M. Salvado; M. Ferreira; *J. Mater. Chem.*, **2015**, *15*, 5099-5111.
2. L. Ye; Y. Zhang; C. Song; Y. Li; B. Jiang; *Mater. Lett.*, **2017**, *188*, 316-318.
3. F. Chi; Y. Zeng; C. Liu; D. Liang; Y. Li; R. Xie; N. Pan; C. Ding; *Results Phys.*, **2020**, *18*, 103315.
4. F. Chi; Y. Zeng; C. Liu; *Optik*, **2020**, *224*, 165501.
5. K.S. Campos; G.F.B. L. e Silva; E.H.M. Nunes; A.M.A. Silva; G.A. Bestard; W.L. Vasconcelos; *Ceram.*, **2019**, *45*, 8626-8633.
6. D. Wang; G. P. Bierwagen; *Prog. Org. Coat.*, **2009**, *64*, 327-338.
7. S. Dalbin; G. Maurin; R.P. Nogueira; J. Persello; N. Pommier; *Surf. Coat. Technol.*, **2005**, *194*, 363-371.
8. A.S.H. Makhlof; *Qatar Foundation Annual Research Forum*, **2013**, Volume Issue 1, HBKU Press.
9. E. Volentiru; M. Nyári; G. Szabó; Z. Hórvölgyi; L. M. Mureșan; *Period. Polytech. Chem. Eng.*, **2014**, *58*, 61-66.
10. N. Cotolan; S. Varvara; E. Albert; G. Szabó; Z. Hórvölgyi; L.M. Mureșan; *Cor. Eng. Sci. Technol.*, **2016**, *51*, 373-382.
11. A.S. Hamdy; F. Alfossail; Z. Gasem; *Electrochim. Acta*, **2013**, *107*, 518-524.
12. E. Albert; N. Cotolan; N. Nagy; Gy. Sáfrán; G. Szabó; L.M. Mureșan; Z. Hórvölgyi; *Microporous Mesoporous Mater.*, **2015**, *206*, 102-113.
13. G. Szabó; E. Albert; J. Both; L. Kócs; Gy. Sáfrán; A. Szöke; Z. Hórvölgyi; L.M. Mureșan; *Surf. Interfaces*, **2019**, *15*, 216-223.

14. A.A. Nazeer; M. Madkour; *J. Mol. Liq.*, **2018**, 253, 11-22.
15. X. Wang; W. Wang; A. Liu; W. Fan; R. Ding; H. Tian; P. Han; W. Li; *Colloids Interface Sci. Commun.*, **2018**, 27, 11-17.
16. M. Montemor; *Surf. Coat. Technol.*, **2014**, 258, 17-37.
17. C.I. Idumah; C.M. Obele; E.O. Emmanuel; A. Hassan; N. Azikiwe; *Surf. Interfaces*, **2020**, 100734.
18. N.Y. Abu-Thabit; A.S. Hamdy; *Surf. Coat. Technol.*, **2016**, 303, 406-424.
19. J. Votava; V. Kumbář; A. Polcar; M. Fajman; *Acta Technol. Agric.*, **2020**, 23, 7-11.
20. J.L. Hutter; J. Bechhoefer; *Rev. Sci. Instrum.*, **1993**, 64, 1868-1873.
21. J.E. Sader; J.W. Chon; P. Mulvaney; *Rev. Sci. Instrum.*, **1994**, 70, 3967-3969.
22. M.P. Gomes, I. Costa; N. Pébère; J.L. Rossi; B. Tribollet; V. Vivier; *Electrochim. Acta*, **2019**, 306, 61-70.
23. M. Stern; A.L. Geary; *J. Electrochem. Soc.*, **1957**, 104, 56.
24. R.B. Vignesh; T.N.J.I. Edison; M. G. Sethuraman; *Mater. Sci. Technol.*, **2014**, 30, 814-820.
25. B. Xue; M. Yu; J. Liu; J. Liu; S. Li; L. Xiong; *J. Alloys Compd.*, **2017**, 725, 84-95.

